IEEE CAT. NO. 97CH36037
Copyright Reg. ISSN 0149-645X

1997 IEEE MTT-S INTERNATIONAL MICROWAVE SYMPOSIUM DIGEST

Volume 2

June 8 - 13, 1997
Colorado Convention Center
Denver, Colorado

CD-ROM Editor
Chris Jelks

Digest Editor
Gerhard A. Koepf

Co-Editors
Don Huebner
Joseph J. Donovan

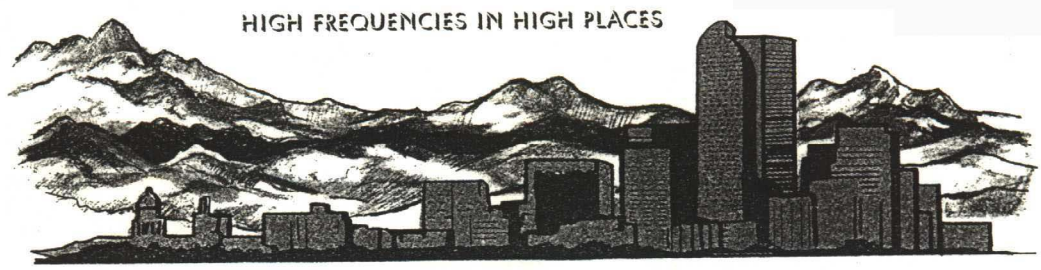

1997 Microwave Symposium Technical Program Schedule

Session WE1A

Nonlinear Modeling and Analysis

8:00 am–9:40 am **Room A201** **Wednesday, June 11, 1997**

Chair: J.C.M. Hwang, Lehigh University

Session WE1B

Passive Components II

8:00 am–9:40 am **Room A207** **Wednesday, June 11, 1997**

Chair: E.J. Denlinger, David Sarnoff Research Center

Session WE1C
Millimeter Wave Devices and Components

8:00 am–9:40 am **Room A102** **Wednesday, June 11, 1997**

Chair: P. Smith, Sanders, a Lockheed Martin Co.
Co-Chair: M. Matloubian, Hughes Research Labs

Session WE1D
Digital Microwave Circuits

8:00 am–9:40 am **Room A101** **Wednesday, June 11, 1997**

Chair: A. Oki, TRW

Session WE1E
New Leakage Effects in Planar Guiding Structures

8:00 am–9:40 am **Room A108** **Wednesday, June 11, 1997**

Chair: A.S. Omar, Technical University Hamburg, Germany
Co-Chair: N.K. Das, Polytechnic University

Session WE2A
Packaging and Interconnect Technologies

10:10 am–11:50 am **Room A201** **Wednesday, June 11, 1997**

Chair: J. Pavio, Motorola
Co-Chair: M. Harris, Georgia Institute of Technology

Session WE2B
High Power Sources and Control Components

10:10 am–11:50 am **Room A207** **Wednesday, June 11, 1997**

Chair: J. Goel, TRW

Session WE2C
Millimeter and Sub-Millimeter Waves:
J.C. Bose Memorial Session

10:10 am–11:50 am **Room A102** **Wednesday, June 11, 1997**

Session Chair: K. Agarwal, Texas Instruments
Co-Chair: J.W. Dees, Georgia Institute of Technology

Session WE2D
Phased Arrays

10:10 am–11:50 am **Room A101** **Wednesday, June 11, 1997**

Chair: M. Thursby, Florida Institute of Technology

Session WE2E
Guided Waves and Discontinuity Effects

10:10 am–11:50 am **Room A108** **Wednesday, June 11, 1997**

Chair: M. Dydyk, Motorola
Co-Chair: S. El-Ghazaly, Arizona State University

Session WE3A
Advanced CAD Methodologies

1:20 pm–3:00 pm **Room A201** **Wednesday, June 11, 1997**

Chair: R.M. Biernacki, Optimization Systems Associates
Co-Chair: M.D. Abouzahra, MIT Lincoln Laboratory

Session WE3B
Frequency Converters and Mixers

1:20 pm–3:00 pm **Room A207** **Wednesday, June 11, 1997**

Chair: B.E. Sigmon, Motorola SSTG, Inc.

Session WE3C
Quasi-Optical Amplifiers

1:20 pm–3:00 pm **Room A102** **Wednesday, June 11, 1997**

Chair: D. Rutledge, California Institute of Technology

Session WE3D
Active and Planar Filters

1:20 pm–3:00 pm **Room A101** **Wednesday, June 11, 1997**

Chair: D. Swanson, Watkins-Johnson

ANALYSIS OF ELECTROTHERMAL TRANSIENTS AND DIGITAL SIGNAL PROCESSING IN ELECTRICALLY AND THERMALLY NONLINEAR MICROWAVE CIRCUITS

Vittorio RIZZOLI (1), Franco MASTRI (2), Andrea NERI (3), and Alessandro LIPPARINI (1)

(1) Dipartimento di Elettronica, Informatica e Sistemistica, University of Bologna, Villa Griffone, 40044 Pontecchio Marconi, Bologna - ITALY
(2) Dipartimento di Ingegneria Elettrica, Viale Risorgimento 2, 40136 Bologna - ITALY
(3) Fondazione Ugo Bordoni, Villa Griffone, 40044 Pontecchio Marconi, Bologna - ITALY

ABSTRACT

The paper introduces a new approach to the analysis of nonlinear circuits containing temperature-dependent devices and excited by slowly modulated microwave carriers. For best accuracy and efficiency, the different dynamics of electrical and thermal phenomena are exploited. The electric circuit is simulated by a sequence of HB analyses of equal size, driven by an exact HB analysis loop for the thermal circuit.

INTRODUCTION

The steadily increasing importance of personal communication systems is stimulating the need for CAD techniques that can efficiently simulate nonlinear circuits and subsystems driven by digitally modulated RF/microwave carriers. In addition, the ability to evaluate the transient behavior of nonlinear circuits is also of considerable interest in a number of more traditional microwave engineering problems such as pulsed-RF operation of power circuits, phase acquisition in PLL's, oscillator and amplifier turnon, and so forth. From a CAD viewpoint, all these applications are special cases of a general simulation problem consisting in the analysis of nonlinear circuits supporting high-frequency quasi-periodic waveforms modulated by relatively low-frequency (possibly digital) signals. While a natural approach to this problem would be time-domain analysis, harmonic-balance (HB) with time-varying phasors has been independently proposed by several research groups [1] - [3] as a more efficient alternative. With these methods, microwave steady-state analysis is decoupled from envelope analysis, so that the well-known efficiency of HB techniques can be fully exploited. One important aspect of circuit operation that has not been taken into account until now in this class of simulations is the effect of device self-heating. Under modulated-RF drive, the active device temperatures are time-dependent, and may exhibit complex waveforms in relation with the RF regime, the shape of the signal envelopes, and the device thermal properties. In turn, this may have a major influence on the circuit performance, especially for power circuits. Very well-known examples are amplitude and phase droop in pulsed power amplifiers, but intermodulation as well may be affected by self-heating, even in simple multitone operation [4]. Thus for example it can be expected that thermal effects may give a contribution to the spectral regrowth and the adjacent-channel interference generated by nonlinear power amplifiers. In addition, the accurate evaluation of the time-dependent dissipated heat is by itself an information of primary importance for the design of some kind of communication equipment, such as portable transceivers. Thus the extension of ordinary HB with variable phasors [1] - [3] to cover electrothermal analysis is certainly worthwhile.

This task is accomplished here by an efficient frequency-domain technique based on a modified version of the modulation-oriented harmonic-balance (MHB) method introduced in [3]. Each active device is described by a nonlinear thermal equivalent circuit consisting of a resistance and a capacitance, and the heat sinking mechanism is simulated by a thermal transmission line [5]. The electrical state variables (SV) of the microwave circuit are described by truncated Fourier series with time-dependent phasors. The time-dependent device temperatures are described by ordinary Fourier expansions. The unknowns are determined by simultaneously solving two coupled nonlinear systems generated by the MHB technique [3] for the microwave circuit, and by the ordinary HB for the thermal circuit. Good numerical efficiency is achieved making use of a hierarchical solution algorithm. The capabilities of the new simulation technique are demonstrated by the electrothermal analysis of a nonlinear power amplifier driven by an 800 MHz carrier with $\pi/4$-DQPSK modulation.

THE ELECTROTHERMAL ANALYSIS ALGORITHM

Let us assume that the temperature-dependent nonlinear subnetwork consists of a collection of multiport semiconductor devices which are thermally isolated from each other, and that the electrical behavior of a generic device is essentially determined by one thermal state variable. This variable is expressed as $T_A + DT_D(t)$, where T_A is the known ambient temperature and $DT_D(t)$ is the excess temperature. The extension to the case of thermally coupled devices (or, equivalently, of devices requiring more than one thermal SV) is possible The electric nonlinear subnetwork can be described by the set of parametric equations

$$\mathbf{v}(t) = \mathbf{u}\left[\mathbf{x}(t),\ \frac{d\mathbf{x}}{dt},\ \mathbf{x_d}(t),\ T_A + \mathbf{DT_D}(t)\right]$$
$$\mathbf{i}(t) = \mathbf{w}\left[\mathbf{x}(t),\ \frac{d\mathbf{x}}{dt},\ \mathbf{x_d}(t),\ T_A + \mathbf{DT_D}(t)\right] \qquad (1)$$

where $\mathbf{v}(t)$, $\mathbf{i}(t)$ are vectors of voltages and currents at the device ports, $\mathbf{x}(t)$ is a vector of electrical SV, and $\mathbf{x_d}(t)$ is a vector of time-delayed electrical SV, i e., $x_{di}(t) = x_i(t - \tau_i)$, τ_i being a time constant. $\mathbf{v}(t)$, $\mathbf{i}(t)$, $\mathbf{x}(t)$ have the same size n_D, equal to the total number of device ports. $\mathbf{DT_D}(t)$ is the vector of the device excess temperatures, and its size N_D equals the number of devices. (1) can easily accomodate advanced electrothermal models of microwave devices [6] and are thus sufficient for our present purposes; however, the generalization of the algorithm to more complex models including higher-order derivatives is straightforward [3]. The heat flow from each device active region to the ambient is modeled by a thermal transmission line (TL) of the kind shown in fig. 1. In this figure, D is the device node, B is the backplane metalization node, and A is the ambient node. Each R-C cell is representative of a section of the physical heat sinking structure,

0-7803-3814-6/97/$5.00 © IEEE

such as a soldering layer, a carrier, and the like. The TL can be analyzed by a dynamic electrical analogy based on the correspondence between heat flow (here represented by the symbol "q") and electric current, excess temperature and voltage. From fig. 1 we obtain the thermal equations of a generic device:

$$DT_B(t) = DT_D(t) + \gamma_D\,\theta_D[DT_D(t), DT_B(t)]\,\frac{dDT_D(t)}{dt} - \theta_D[DT_D(t), DT_B(t)]\,q(t)$$
$$q_B(t) = \gamma_D\,\frac{dDT_D(t)}{dt} - q(t) \qquad (2)$$

where γ_D, θ_D are the device thermal capacitance and thermal resistance, $q(t)$ is the power dissipated in the device, and $DT_B(t)$ is the backplane temperature. The thermal resistance is temperature-dependent and can be explicitly formulated by means of the Kirchhoff transform [5]. The small dependence on temperature of the specific heat is practically negligible, so that the thermal capacitance is considered linear. Note that (2) have the same canonical form as (1), with thermal state variables $DT_D(t)$, $DT_B(t)$. The thermal nonlinear subnetwork is active, however, since it contains the state-dependent source $q(t)$.

The electrical and thermal linear subnetworks may be described by frequency-domain equations of the form

$$\mathbf{I}(\omega) + \mathbf{Y}(\omega)\,\mathbf{V}(\omega) + \mathbf{Y_F}(\omega)\,\mathbf{F}(\omega) = \mathbf{0} \qquad (3)$$

$$\mathbf{Z_T}(\omega)\,\mathbf{Q_B}(\omega) + \mathbf{D_B}(\omega) = \mathbf{0} \qquad (4)$$

In (3) $\mathbf{Y}(\omega)$ is the admittance matrix at the device ports when all source ports are short-circuited, $\mathbf{Y_F}(\omega)$ is the forward trans-admittance matrix from the source ports to the device ports, and $\mathbf{F}(\omega)$ is the vector of free sinusoidal voltage sources of angular frequency ω (*forcing terms*) connected to the source ports. Source and load resistances are included in the linear subnetwork. In (4) $\mathbf{Z_T}(\omega)$ is the diagonal matrix of the input thermal impedances of all TLs, and $\mathbf{Q_B}(\omega)$, $\mathbf{D_B}(\omega)$ are vectors of phasors of the spectral components of $q_B(t)$, $DT_B(t)$, for all devices at frequency ω. $\mathbf{Z_T}(\omega)$ is computed from fig. 1 by conventional linear circuit methods. The linear and nonlinear subnetwork equations (1) - (4) must be simultaneously solved (for all nonlinear devices) by the electrothermal analysis.

Let us now assume that the forcing terms are quasi-periodic microwave signals slowly modulated in amplitude and phase by baseband signals, i.e.,

$$\mathbf{f}(t) = \sum_{\mathbf{k}} \mathbf{F_k}(t)\,\exp(j\Omega_{\mathbf{k}}t) \qquad (5)$$

where $\Omega_{\mathbf{k}}$ is a generic intermodulation (IM) product of a set of RF/microwave fundamental frequencies ω_i, and the complex modulation laws $\mathbf{F_k}(t)$ are slowly varying with time. With the usual HB notation, $\mathbf{k}$ is a vector of integer harmonic numbers. The state vector $\mathbf{x}(t)$ has an expression similar to (5), with $\mathbf{F_k}(t)$ replaced by $\mathbf{X_k}(t)$. Since the thermal time constants of microwave semiconductor devices are normally large with respect to the RF period, the time-dependent device temperatures will only contain the baseband terms ($\mathbf{k} = \mathbf{0}$). Without loss of generality, we shall assume that all the $\mathbf{F_k}(t)$, and thus $\mathbf{X_k}(t)$, $\mathbf{DT_D}(t)$, $\mathbf{DT_B}(t)$ as well, are periodic or quasi-periodic. This allows the spectral properties of the modulation laws to be evaluated by the Discrete Fourier Transform (DFT).

Now let the modulation laws be sampled at a finite number of uniformly spaced time instants t_n ($1 \le n \le N$), that will be referred to as the modulation-law sampling (MS) instants. In order to find the electric nonlinear subnetwork response to $\mathbf{x}(t)$, we introduce a quasi-stationary approximation. We assume that the time constants of the microwave circuit are so short, that its electrical regime under modulated-RF drive can be described as a sequence of RF steady states [1] - [3], each associated with the set of values that the modulation laws and the device excess temperatures take on at a specific MS instant. Making use of (5) we get [3]

$$\frac{d\mathbf{x}(t)}{dt} = \sum_{\mathbf{k}} \left[j\Omega_{\mathbf{k}}\mathbf{X_k}(t) + \frac{d\mathbf{X_k}(t)}{dt}\right]\exp(j\Omega_{\mathbf{k}}t)$$
$$\mathbf{x_d}(t) \approx \sum_{\mathbf{k}} \exp(-j\Omega_{\mathbf{k}}\mathbf{T})\left[\mathbf{X_k}(t) - \mathbf{T}\,\frac{d\mathbf{X_k}(t)}{dt}\right]\exp(j\Omega_{\mathbf{k}}t) \qquad (6)$$

where $\mathbf{T}$ is the diagonal matrix of the time delays τ_i. The computation of (6) requires the derivatives $d\mathbf{X_k}/dt$ which can be evaluated at the MS instant t_n by one-sided multipoint incremental rules of the general form

$$\left.\frac{d\mathbf{X_k}(t)}{dt}\right|_{t=t_n} \approx \sum_{m=0}^{M} a_m\,\mathbf{X_k}(t_{n-m}) \qquad (7)$$

where the coefficients a_m are explicitly listed in many mathematical handbooks. The accuracy of the derivatives, and thus of the MHB analysis, increases with M. However, it has been found that small values of M (say, $M \le 2$) are sufficient to obtain very satisfactory results in most practical cases. By means of (6), (7), and of the quasi-stationary approximation, the harmonics of (1) at each MS instant, namely $\mathbf{U_k}(t_n)$, $\mathbf{W_k}(t_n)$, can be computed by a multidimensional DFT as a function of $\mathbf{X_h}(t_{n-m})$ (for all $\mathbf{h}$ and $0 \le m \le M$) [3].

Under the same assumptions, if Ω is an angular frequency falling inside the band of the modulation laws, a frequency change by Ω will produce a very small modification of the microwave circuit admittance. Thus in the neighborhood of each $\Omega_{\mathbf{k}}$ the admittance matrices $\mathbf{Y}(\omega)$, $\mathbf{Y_F}(\omega)$ may be approximated by truncated Taylor expansions. By combining such expansions with the linear subnetwork equations and replacing the harmonics $\mathbf{U_k}(t_n)$, $\mathbf{W_k}(t_n)$ of (1) for $\mathbf{I}(\omega)$, $\mathbf{V}(\omega)$ in (3), we obtain a nonlinear system for the SV harmonics at a generic MS instant t_n. The mathematical developments are similar to those reported in [3], and will not be repeated here. An important difference, however, is that here we make use of the one-sided formula (7) for the derivatives, instead of the two-sided formula used in [3]. Each MS instant is then coupled to a finite number of other MS instants that precede it in time. If the real and imaginary parts of the HB errors (for all $\mathbf{k}$) are stacked into a real electrical error vector $\mathbf{E_n}$, the electrical HB system for $t = t_n$ may then be symbolically stated in the form

$$\mathbf{E_n}[\mathbf{Z_n}, \mathbf{Z_{n-1}}, \ldots, \mathbf{Z_{n-2M}}, \{\textit{thermal unknowns}\}] = \mathbf{0} \qquad (8)$$

where $\mathbf{Z_n}$ is the vector of real and imaginary parts of the $\mathbf{X_k}(t_n)$ (for a fixed n and all $\mathbf{k}$). The entries of $\mathbf{Z_n}$ (for all n) represent the electrical unknowns. The set of all electrical unknowns will be denoted by $\mathbf{Z}$. Note that the nonlinear operator $\mathbf{E_n}[\cdot]$ is obviously temperature-dependent, as well, so that the system

(8) also contains the thermal unknowns. However, the latter are different in nature from the electrical unknowns, as explained by the following discussion.

The quasi-stationary assumption leading to (8) cannot be used in the nonlinear analysis of the thermal circuit. This is due to the fact that the thermal circuit time constants are rather long, ranging from several μs (for the active devices) to several ms (for a real heat sink), and thus typically have the same order of magnitude as the time constants of the modulation laws. For instance, in the NADC system [7] the RF carrier is modulated at a rate of 49 kb/s, so that the bit interval is about 20.4 μs. Thus the thermal circuit electrical regime is fully dynamic, and must be analyzed by a rigorous HB approach. Since by assumption the modulation laws are quasi-periodic, they can be expressed by multiple Fourier expansions of the form

$$\mathbf{F}_k(t) = \sum_s \mathbf{F}_{s,k} \exp(j\Omega_s' t) \tag{9}$$

where the Ω_s' are IM products of a set of baseband fundamental frequencies ω_i'. All time-dependent thermal quantities may be represented by similar expansions. In particular, for the N_D-vectors of the peak and backplane device excess temperatures, $\mathbf{DT_D}(t)$, $\mathbf{DT_B}(t)$, the s-th harmonics will be denoted by $\mathbf{D_{Ds}}$, $\mathbf{D_{Bs}}$. The vector containing the real and imaginary parts of all harmonics $\mathbf{D_{Ds}}$, $\mathbf{D_{Bs}}$, will be denoted by $\mathbf{D}$. The entries of $\mathbf{D}$ are the thermal unknowns.

At the MS sampling instant t_n ($1 \le n \le N$), the power dissipated in the r-th device ($1 \le r \le N_D$) is given by

$$q_r(t_n) = \mathrm{Re}\left[\mathbf{U_0}^T(t_n)\,\mathbf{W_0}(t_n) + \frac{1}{2}\sum_{k\neq 0}\mathbf{U_k}^T(t_n)\,\mathbf{W_k}^*(t_n)\right]^{(r)} \tag{10}$$

where the superscript (r) indicates that the vector products are only extended to the voltage and current harmonics at the r-th device ports. A Fourier expansion of the form (9) for $q_r(t)$ may then be computed by the DFT. The formulation of the thermal HB equations is now straightforward, and follows the same guidelines as for a conventional HB analysis [8]. The real and imaginary parts of the thermal HB errors are stacked into a real thermal error vector $\mathbf{E_T(Z, D)}$, so that the electrothermal MHB solving system may be written in the form

$$\begin{cases} \mathbf{E}_n[\mathbf{Z}_n, \mathbf{Z}_{n-1}, \ldots, \mathbf{Z}_{n-2M}, \mathbf{D}] = \mathbf{0} \\ (1 \le n \le N) \\ \\ \mathbf{E_T}(\mathbf{Z}, \mathbf{D}) = \mathbf{0} \end{cases} \tag{11}$$

(11) is a system of $N_U = Nn_D(2n_H + 1) + 2N_D(2n_T + 1)$ real equations in as many real unknowns, where n_H, n_T are the numbers of IM products used to describe the microwave steady-state regime and the time-dependent thermal quantities.

SOLUTION OF THE NONLINEAR SYSTEM

In many practical cases (such as for digitally modulated carriers) the number of MS instants may be quite large, so that the number of unknowns may climb up to several tens of thousands or more [1] - [3]. Thus in order to avoid exceedingly large CPU times, a clever solution strategy for the system (11) is needed. It turns out that this system is ideally suited for the application of the hierarchical technique introduced in [9]. n_T is normally less than N/2, but can often be further reduced if the fine details of the temperature waveforms are not of specific interest. In addition, $N_D \le n_D$. Thus the size of the thermal subsystem in (11) is much smaller than N_U. Following [9], we may assign to the thermal subsystem the role of master system, or equivalently solve the nonlinear system

$$\mathbf{E_T}[\mathbf{Z}(\mathbf{D}), \mathbf{D}] = \mathbf{0} \tag{12}$$

where $\mathbf{Z}(\mathbf{D})$ is the solution of the electrical subsystem for a given $\mathbf{D}$. In turn, the electrical subsystem can be efficiently solved thanks to its very peculiar structure. As a matter of fact, for a given set of thermal unknowns, (8) can be viewed as a real system of $n_D(2n_H + 1)$ equations in as many unknowns (the entries of $\mathbf{Z}_n$), with $\mathbf{Z}_{n-1}$, ..., $\mathbf{Z}_{n-2M}$ playing the role of parameters. Thus with a suitable intialization, the electrical subsystem can be solved as a sequence of N independent ordinary HB systems of size $n_D(2n_H + 1)$.

In practice, (12) is solved by a Newton iteration starting from $\mathbf{D} = \mathbf{0}$. For a given $\mathbf{D}$ the device excess temperatures can be evaluated at all the MS instants. The electrical subsystem may then be solved starting from the solutions obtained at the previous iteration ($\mathbf{Z} = \mathbf{0}$ at startup). At the first MS instant t_1, an ordinary HB analysis is carried out. At the MS instants t_m ($2 \le m \le 2M$) the expressions (7) of the derivatives are suitably simplified (i.e., by reducing M), so that the computation only requires already available information from the preceding MS instants. For $n > 2M$ the standard system (8) is sequentially solved for increasing values of n. At the end of this process, the heat sources are evaluated by (10) (for all r, n) and Fourier transformed, which provides the forcing terms of the thermal HB equations. The thermal HB errors may then be computed. The Jacobian matrix of (12) is exactly evaluated by algorithms similar to those discussed in [8], [9]. Since (12) is only mildly nonlinear, 2-3 iterations with respect to the thermal unknowns are usually sufficient to achieve convergence, so that the overall solution process is numerically efficient.

AN EXAMPLE OF APPLICATION

As an example of application, we consider the electrothermal analysis of a power amplifier driven by a digitally modulated carrier. The carrier frequency is 835 MHz and the modulation format is π/4-DQPSK according to the NADC standard [7]. The amplifier consists of a simple class-A FET stage operated at 4 dB gain compression, and the active device is modeled after [6]. The device is assumed to be mounted in a microstrip package, whose ground plane is soldered to a metal heat sink of finite size. Three layers representing the package, the solder, and the finite heat sink, are thus included in the thermal TL between the device backplane and the ambient. The thermal conductivity of GaAs is assumed to be proportional to $T^{-1.2}$ [5]. The baseband bit stream is described as a periodic sequence of 512 bits with a bit rate of 49 kb/s. Figs. 2, 3 show the input and output normalized power spectra of the modulated carrier, for an input power of +23.25 dBm on the useful channel. The output spectrum is shifted by an amount equal to the amplifier gain for ease of comparison. The spectral regrowth of the output signal due to IM distortion in the power amplifier is evident from these figures. The power gain and power-added efficiency of the amplifier are obviously influenced by the device self-heating. With digital modulation and +23.25 dBm input power on the useful channel, the gain and efficiency values with the device at ambient temperature (290 °K) are G = 7.4 dB, η = 34.4 %. On the other hand, when self-heating is accounted for the gain drops to G = 6.1 dB, with a power-added efficiency η = 27.7 %. Fig. 4 shows the

in-phase and quadrature components of the output modulation laws and the FET temperature waveform $T_A + DT_D(t)$ in a 64-bit slot extracted from the main sequence. The FET thermal time constant is about 120 μs at 290 °K. The analysis makes use of 4 sampling points per bit and 4 carrier harmonics plus d.c., so that N = 2048, and the number of electrical unknowns is 36864. n_T = 512 thermal harmonics are used, so that the number of thermal unknowns is 2050, and N_U = 38914. The CPU time is 1136 seconds on an HP 755 workstation.

ACKNOWLEDGMENTS

This work was partly sponsored by the Italian Ministry of University and Scientific Research (MURST) and by the Istituto Superiore delle Poste e delle Telecomunicazioni (ISPT).

REFERENCES

[1] D. Sharrit, "New circuit simulation analysis methods for communication systems", *Digest of IEEE MTT-S Workshop WMFA: Nonlinear CAD*, San Francisco, June 1996, pp. 29-41.

[2] E. Ngoya and R. Larchevèque, "Envelop transient analysis: a new method for the transient and steady state analysis of microwave communication circuits and systems", *1996 IEEE MTT-S Int. Microwave Symp. Digest*, San Francisco, June 1996, pp. 1365-1368.

[3] V. Rizzoli, A. Neri, and F. Mastri, "A modulation-oriented piecewise harmonic-balance technique suitable for transient analysis and digitally modulated signals", *Proc. 26th European Microwave Conf.*, Prague, Sept. 1996, pp. 546-550.

[4] K. Lu *et al.*, "Low-frequency dispersion and its influence on the intermodulation performance of AlGaAs/GaAs HBT", *1996 IEEE MTT-S Int. Microwave Symp. Digest*, San Francisco, June 1996, pp. 1373-1376.

[5] J. V. DiLorenzo and D. K. Khandelval, *GaAs FET Principles and Technology*. Dedham: Artech House, 1982.

[6] V. Rizzoli *et al.*, "An electrothermal functional model of the microwave FET suitable for nonlinear simulation", *Int. J. Microwave Millimeterwave Comp. Aided Eng.*, Vol. 5, Mar. 1995, pp. 104-121.

[7] J. D. Gibson (*ed.*), *The Mobile Communications Handbook*. Boca Raton: CRC Press, 1996.

[8] V. Rizzoli *et al.*, "Frequency-domain analysis of electrically and thermally nonlinear microwave circuits", *Proc. 22nd European Microwave Conf.*, Helsinki, Aug. 1992, pp. 1097-1102.

[9] V. Rizzoli, F. Mastri, and D. Masotti, "A hierarchical harmonic-balance technique for the efficient simulation of large-size nonlinear microwave circuits", *Proc. 25th European Microwave Conf.*, Bologna, Sept. 1995, pp. 615-619.

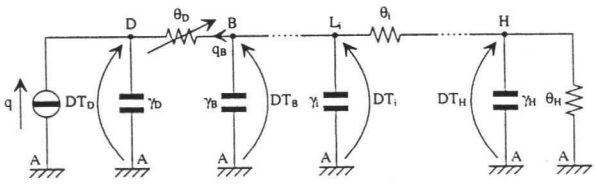

Fig. 1 - Thermal transmission-line model of the heat flow from an active device.

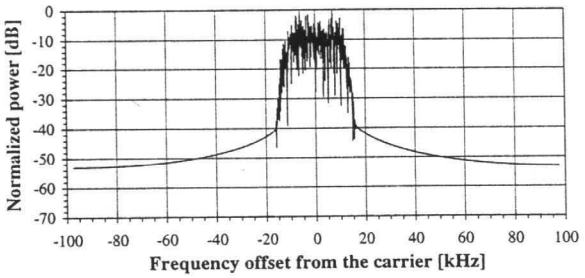

Fig. 2 - Input power spectrum.

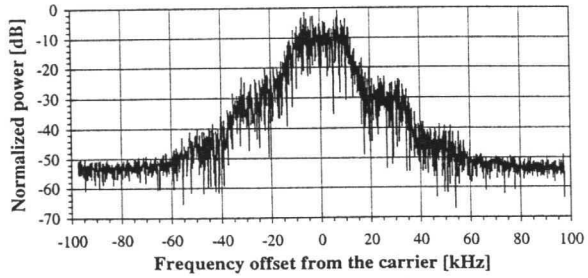

Fig. 3 - Output power spectrum.

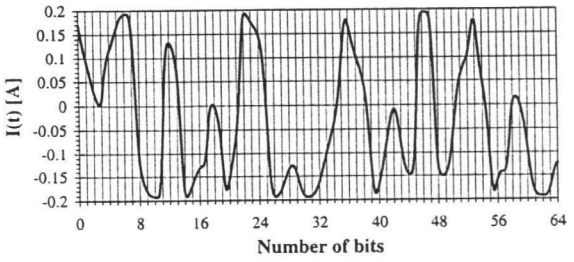

Fig. 4a - In phase modulation law of the load current.

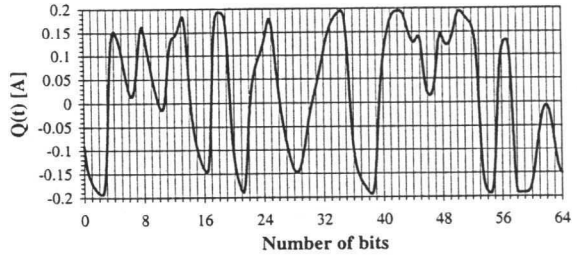

Fig. 4b - Quadrature modulation law of the load current.

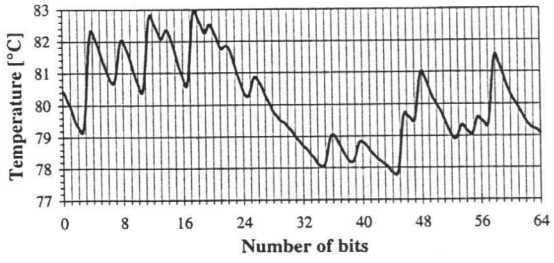

Fig. 4c - Peak device temperature.

THE EFFECT OF A VARIATION IN TONE SPACING ON THE INTERMODULATION PERFORMANCE OF CLASS A & CLASS AB HBT POWER AMPLIFIERS

Paul M. McIntosh and Christopher M. Snowden
Dept Electronic & Electrical Engineering
The University Of Leeds, Leeds, LS2 9JT, United Kingdom

Abstract

The first investigation into the effect of frequency separation on the intermodulation distortion performance of Heterojunction Bipolar Transistor (HBT) power amplifiers is reported. The measured results show that the frequency spacing between the two input tones affects the intermodulation distortion performance of Class AB power amplifiers, but not Class A power amplifiers.

1. Introduction

HBTs are becoming a very popular choice of device for use in microwave power amplifiers [1,2] owing to characteristics such as high gain, linearity, and high output power. The intermodulation distortion performance of these devices has been investigated [3] and it has been proposed that they offer superior intermodulation distortion performance [4].

Highly linear power amplifiers are a vital requirement in multi-carrier communication systems where the carrier signals may be closely spaced in frequency, and it has been suggested that HBT power amplifiers may be able to address this requirement [5]. The thermal performance of power HBTs is known to limit device operation [6,7] and it has been further proposed that the thermal aspects of HBT operation can affect the intermodulation distortion performance [8]. The frequency spacing between the two input tones can affect the intermodulation distortion of an HBT biased in Class AB [8], and this paper extends the work on intermodulation distortion performance in power amplifiers by examining the role of bias conditions and their interaction with thermal operation. The work presented here examines for the first time the effect of a variation in frequency separation of the two input tones on the third order intermodulation distortion (IM_3) performance of a Class A and a Class AB HBT power amplifier. The frequency spacing (Δf) used for IM_3 measurements is usually between 1 MHz and 10 MHz. This work uses a range of different Δf in measurements and simulations to fully characterise the IM_3 performance of HBT power amplifiers.

2. Theoretical Background and Power Amplifier Simulations

The work discussed in [8] has shown that the non-linearity of the Class AB operation results in mixing products that fall within the thermal frequency response of the device causing a change in the thermal operation which results in an increase in the power of the IM_3 products. This means that HBT power amplifiers where Δf falls within this thermal frequency response have to be characterised carefully and this paper examines the intermodulation distortion performance of both Class A and Class AB HBT power amplifiers with values of Δf between 2 kHz and 1 MHz.

0-7803-3814-6/97/$5.00 © IEEE

Isothermal power amplifier simulations using an equivalent circuit model [9] which does not contain a thermal model have been carried out on a Class A power amplifier. This model describes a power HBT and a simulated load-pull was carried out to determine the optimum reflection coefficients to give maximum power gain. The IM_3 performance of this circuit was simulated using two different input tone frequency spacings. The first simulation was carried out with a spacing of 1 MHz and the second with a frequency spacing of 2 kHz. The results are shown in **Figure 1** and demonstrate that in the absence of any thermal effects the power of the IM_3 products does not change with a variation in input tone frequency spacing until the amplifier is driven well into the power gain saturation region.

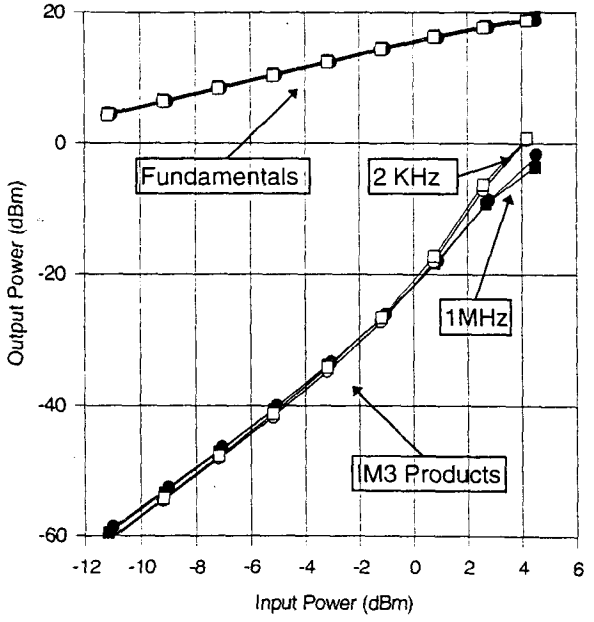

Figure 1 Class A Power Amplifier Simulations with a Variation In Frequency Spacing of the Two Input Tones.
□ ○ $\Delta f = 2$ kHz, ■ ● $\Delta f = 1$ MHz

3. Amplifier Design And Intermodulation Distortion Measurements

The two HBT power amplifiers used in this work were designed using load-pull measurements. A TRL calibration technique [10] was used to allow the measurements to be de-embedded to the plane of the devices used. The load-pull measurements were performed under Class A and Class AB bias conditions at 1.8GHz and from the results the power amplifiers were designed for maximum power gain. Each power amplifier was fabricated on microstrip and external bias Tees were used to provide the power supplies to the transistor. The P_{in}/P_{out} characteristics were measured and using the test setup shown in **Figure 2** the IM_3 performance of each amplifier was measured.

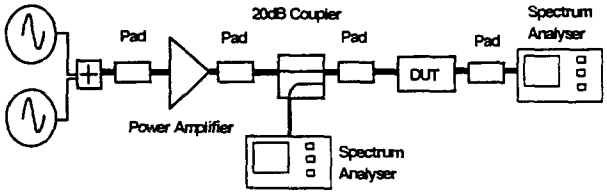

Figure 2 Two-Tone Intermodulation Distortion Measurement Setup

The frequency spacing (Δf) between the two input tones in the first measurement was set at 1 MHz and in the second measurement Δf was reduced to 4 kHz. **Figure 3** shows a typical spectrum analyzer output obtained during the measurements where the IM_3 products can be clearly seen.

4. Measurement Results

Figure 4 shows the output power level of each of the fundamentals and all of the 3rd order products resulting from the non-linear mixing of the two input tones for both the Class A and AB power amplifiers.

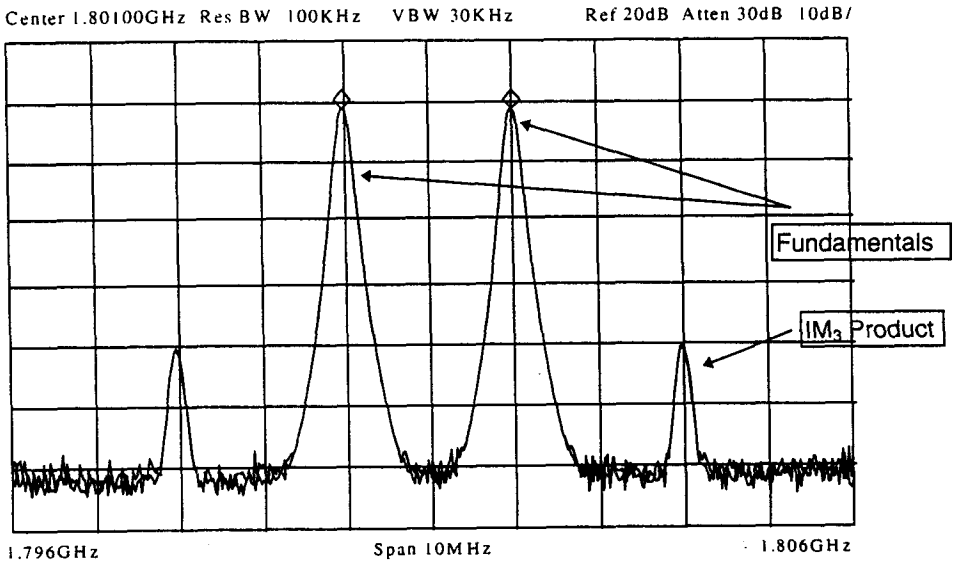

Figure 3 Typical Power Amplifier Spectrum

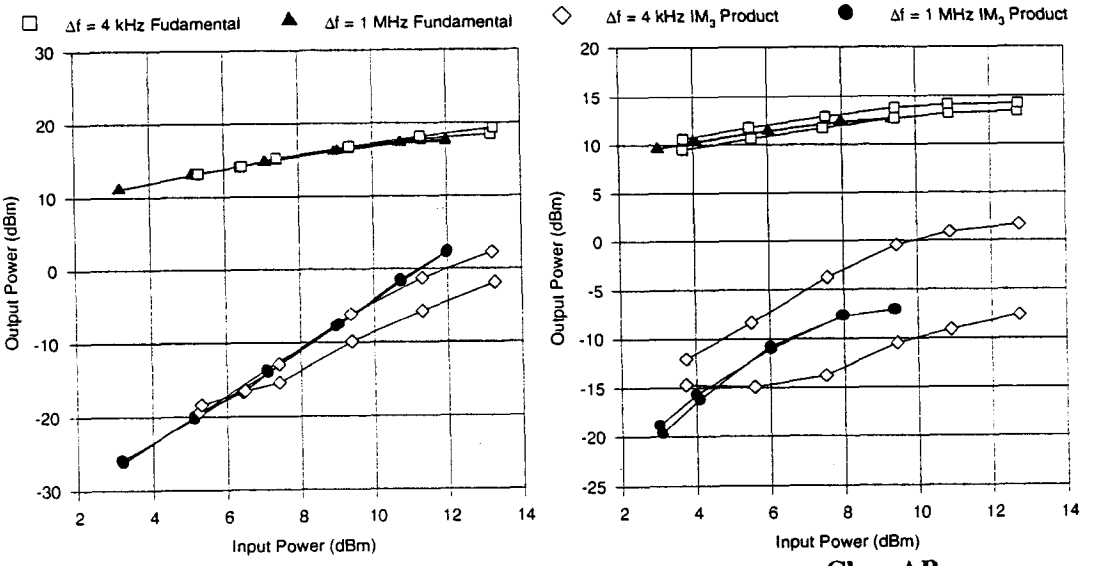

Figure 4 IM_3 Results For The Class A and Class AB HBT Power Amplifier. Fundamentals and all 3rd Order Products are Shown

In the Class A case the variation in Δf does not cause an increase in the power of the third order products. This is probably due to the linear operation of the power amplifier which although generating intermodulation distortion products that fall within the thermal frequency response of the circuit such as (f_2-f_1) product they are not of sufficient power to affect the intermodulation distortion performance. There is some variation in the power of the IM_3 products, but no

increase. The variation is likely to be due to simultaneous phase and amplitude distortion[11]. The Class AB results contrast strongly with the Class A case results and show that when Δf is reduced to 4 kHz the power of the third order products can be increased by between 4 dB and 6.5 dB. This is a significant deterioration in the amplifier's performance and can be attributed to the f_2-f_1 product which falls within the thermal frequency response of the power amplifier causing the bias point to be modulated. This affects the thermal performance of the power amplifier increasing the non-linearity of operation and degrading the IM_3 performance. The comparison between the Class A and AB operation also shows that this change must be device rather than measurement equipment related since it has been seen in one Class of operation, but not in both when an identical test equipment setup has been used.

5. Conclusions

The results show that intermodulation distortion measurements where Δf may be anything between 1 MHz and 10 MHz may not be sufficient to fully describe the IM_3 performance of a Class AB HBT power amplifier which is a common Class of operation chosen by many circuit designers for mobile communications systems. Measurements presented here show that the IM_3 performance of a Class AB amplifier may be up to 6.5 dB worse when the f_2-f_1 product falls within the amplifier's thermal frequency response causing a change in the thermal performance of the power amplifier. There was no reduction seen in the IM_3 performance of a Class A HBT power amplifier showing the linear operation of this Class and demonstrating that the use of a frequency spacing between 1 MHz and 10 MHz in two-tone intermodulation distortion measurements is sufficient to describe the Class A power amplifiers IM_3 performance. The Class A and AB results also show that the change in IM_3 performance is device related rather than test equipment related.

6. Acknowledgments

The authors acknowledge the U.K EPSRC, M/A-COM Corporate Research and Development, U.S.A and Dr K.Lu for his advice.

7. References

[1] G. Ferrel *et al*, "A High Efficiency 10 Watt HBT Power Amplifier Assembly Using Combining Techniques," *IEEE International Microwave Symposium Digest*, pp327-30, 1995.

[2] T. Yoshimasu *et al*, "High Efficiency HBT MMIC Linear Power Amplifier For L-Band Personal Communication Systems," *IEEE Microwave and Guided Wave Lett.*, vol 4, pp65-7, 1994.

[3] S.A Maas, B.L.Nelson and D.L.Tait, "Intermodulation In Heterojunction In Bipolar Transistors", *IEEE Trans. Microwave Theory Tech.*, vol.40,no 3, pp442-448, 1992. *IEEE Trans. Microwave Theory Tech.*, vol.42,no 10, pp1845-50, 1994.

[4] N.L.wang, W.J.Ho and J.A.Higgins, "AlGaAs/GaAs HBT Linearity Characteristics", *IEEE Trans. Microwave Theory Tech.*, vol.42,no 10, pp1845-50, 1994.

[5] W.J.Pratt, "High Linearity HBT Amplifier Targets Multicarrier Systems", *RF Design*, pp47-54, March 1996.

[6] J. A. Higgins, "Thermal Properties of Power HBTs," *IEEE Trans. Electron Devices*, vol.40, pp2171-7, 1993.

[7] W.Liu, S.Nelson, D.G.Hill and A.Khatibzadeh, "Current Gain Collapse In Microwave Multi-Finger Heterojunction Bipolar Transistors Operated At Very High Power Densities", *IEEE Trans. Electron Devices*, vol.40, no 11,pp1917-26, 1993.

[8] K.Lu, P.M.McIntosh,C.M.Snowden and R.D.Pollard, "Low frequency Dispersion and its Effect On The Intermodulation Performance Of AlGaAs/GaAs HBTs", *IEEE International Microwave Symposium Digest*, pp1373-76, 1996.

[9] D.W.Wu, M.Fukuda and Y.H.Yun, "A Novel Extraction Method For Accurate Determination Of HBT Large-Signal Model Parameters", *IEEE International Microwave Symposium Digest*, pp1235-1238, 1995.

[10] Hewlett Packard Aplication Note No. HP 8510-8, "Applying The 8510B TRL Calibration For Non-Coaxial Measurements"

[11] H.Krauss, C.Bostian and F. Raab, "Solid State Radio Engineering", John Wiley & Sons, 1980.

COMPARISON OF HYBRID PI AND TEE HBT CIRCUIT TOPOLOGIES AND THEIR RELATIONSHIP TO LARGE SIGNAL MODELING

Douglas A. Teeter*, Walter R. Curtice**

*Raytheon Electronics, Advanced Device Center, Research Laboratories, 362 Lowell Street, Andover, MA 01810, (508) 470-9402

**W. R. Curtice Consulting, 5 Berkshire Dr, Princeton Junction, NJ 08550, (609) 799-1175

ABSTRACT

Direct comparison between the HBT small signal Tee model and the hybrid pi topology is made to 100 GHz. It is shown that a one to one correspondence exists between the two topologies, but that some of the pi model parameters exhibit a frequency dependence with respect to the Tee model parameters. Using this analysis, an enhanced Gummel Poon large signal model has been developed which extends the model accuracy (usually up to mm-wave) by properly including collector current delay, self heating, and avalanche breakdown. A collection of measured versus modeled results are given.

INTRODUCTION

Most papers dealing with small signal HBT device performance make use of the Tee model topology[1-4]. These papers are written primarily by device developers and researchers extracting models from small signal S parameter data. The Tee model is appealing because all the model parameters can be directly tied to the physics of the device and the model fits S parameter data very well up to mm-wave frequencies. A few papers have dealt with the hybrid pi topology [5-6].

For historical reasons dating back to silicon bipolar transistor development, the Gummel Poon model is used by most bipolar circuit designers. This model is the standard large signal bipolar model available in most circuit simulators (SPICE, LIBRA, MDS, etc.). Thus, for designs which require large signal modeling, such as oscillators, power amplifiers, and mixers, the designer must use the Gummel Poon model. Unfortunately, the Gummel Poon model reduces to the hybrid pi topology under small signal conditions, a different circuit topology from the tee model. Thus, *there is a fundamental difference between the HBT model used by device developers and that used by most circuit designers.*

This paper makes a direct comparison between the pi and tee circuit topologies. It is shown that a one to one correspondence exists between the two circuit topologies. However, the pi model parameters have a frequency dependence which becomes noticeable at high frequencies. For the devices we looked at, this occurs above 30-40 GHz. Both model topologies, when optimized, are shown to give good agreement with measured S parameter data to 50 GHz. The analysis shows that *the standard Gummel Poon large signal model can be satisfactorily used over the usable operating range of the transistor (50 GHz in our case) as long as the collector current delay is properly included in the current generator (many Gummel Poon models available in commercial simulators do not properly include this delay).* A modified Gummel Poon model which properly includes transit time delay has been developed and is described in the paper. The model is completely compatible with the standard Gummel Poon model with the important addition of transit time delay, self heating, and avalanche breakdown.

DISCUSSION

Analysis begins by comparing the pi and tee circuit toplogies. One quickly notices that the only real difference exists between the intrinsic device model, shown in

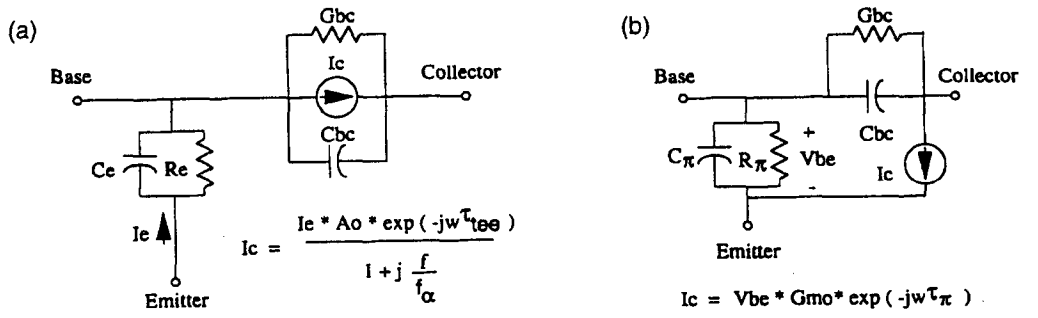

Figure 1. (a)Intrinsic HBT Tee Model, (b) Intrinsic HBT Hybrid Pi Model

0-7803-3814-6/97/$5.00 © IEEE